U·P·O·J

Mechano-active Therapeutic Release to Preserve Subchondral Bone After Nanofracture in a Large Animal

Hannah M. Zlotnick, BS[1,2,3]
Ryan C. Locke, PhD[1,3]
Sanjana Hemdev, BS[1,2,3]
Brendan D. Stoeckl, MS[1,2,3]
Sachin Gupta, MD[1,3]
Ana P. Peredo, BS[1,2,3]
David R. Steinberg, MD[1,3]
James L. Carey, MD, MPH[1,3]
Daeyeon Lee, PhD[4]
George R. Dodge, PhD[1,3]
Robert L. Mauck, PhD[1,2,3]

[1]Department of Orthopaedic Surgery, University of Pennsylvania, Philadelphia, PA

[2]Department of Bioengineering, University of Pennsylvania, Philadelphia, PA

[3]Translational Musculoskeletal Research Center, Philadelphia VA Medical Center, Philadelphia, PA

[4]Department of Chemical and Biomolecular Engineering, University of Pennsylvania, Philadelphia, PA

Introduction

During microfracture, the subchondral bone is perforated to enable the upward migration of marrow cells. While beneficial for repair tissue formation, these subchondral perforations can lead to bony cysts and resorption, compromising the foundation on which the neocartilage forms. To extend the lifetime of cartilage repair and minimize bone damage, smaller diameter, deeper marrow stimulation holes (nanofracture – Nfx) can limit bone resorption[1]. In this study, we aimed to further preserve the subchondral bone after Nfx by locally delivering osteogenic therapeutics to the cartilage-to-bone interface. To do so, we designed mechanically activated microcapsules (MAMCs) applied at the osteochondral interface, and locally release small bioactive agents—triiodothyronine (T3) and ß-glycerophosphate upon mechanical loading. We hypothesized that the delivery of therapeutic MAMCs would reduce bone resorption and stimulate local bone formation at the osteochondral interface, as assessed 1 and 2 weeks post-Nfx.

Methods

Osteogenic assessment

Mesenchymal stromal cell (MSC) pellets (200,000 cells/pellet) were precultured in chondrogenic media with TGF-ß3 (10 ng/mL), administered a single dose of T3 (10 nM) and ß-glycerophosphate (10 mM) (or not for the controls), and further cultured for 2 weeks in chemically defined media, as previously described by Mueller et al[2]. An alkaline phosphatase (AP) assay was performed on collected culture media at the terminal time point.

MAMC fabrication

MAMCs were fabricated as previously described, and osmotically annealed[3]. Sinking behavior was assessed in saline. The mechano-release profiles of the MAMCs were tested in direct compression using an Instron.

Surgical model

Six adult male Yucatan minipigs underwent a unilateral cartilage defect repair procedure. Six 5 mm diameter chondral defects were created in the trochlear groove. The treatment groups included: Nfx alone (n = 2/animal), Nfx + control MAMCs (n = 2/animal), and Nfx + therapeutic MAMCs (n = 2/animal). Therapeutic MAMCs delivered 1.3 ng T3 and 432 µg ß-glycerophosphate to the respective defects. Nanofracture was performed with a 1.2 mm diameter SmartShot® device (2 holes/defect). At the time of surgery, all animals received an intravenous injection of xylenol orange1. The animals were euthanized 1 (N = 3) and 2 (N = 3) weeks post-surgery.

Post-mortem analyses

Osteochondral units were prepared for microcomputed tomography (µCT) scanning. The samples were then cryosectioned to the midplane of each defect, and serially stained (mineral label, tartrate resistant acid phosphatase (TRAP), AP, Toluidine Blue)[4]. The remaining samples were further embedded in paraffin wax, sectioned, and stained.

Statistics

Figure 1A: t-test, Figure 1D, 2C, 2E: ANOVA, Bonferroni corrections. Data shown: mean ± standard deviation.

Results

A single dose of T3 and ß-glycerophosphate increased AP activity of MSC pellets (Figure 1A). These therapeutic agents were selected for encapsulation in MAMCs. Control MAMCs were slightly larger in diameter than the therapeutic MAMCs (Figure 1B). However, the shell thickness to diameter (t/d) ratio of each batch was similar (control: 0.08, therapeutic: 0.06). The MAMCs settled to the bottom surface of a glass vial (2.5 cm depth of saline) within 15 seconds (Figure 1C), and both batches had similar mechano-release profiles (Figure 1D). Post-surgery, all animals were weight-bearing within 2 hours (Figure 2A). All defects were utilized for each outcome (Figure 2B). The therapeutic MAMCs significantly reduced volumetric bone resorption in comparison to Nfx alone (Figure 2C). Interestingly, mineral labeling appeared similar after 1 week, but differences were marked at 2 weeks (Figure 2D). There were significant decreases in label coverage in both

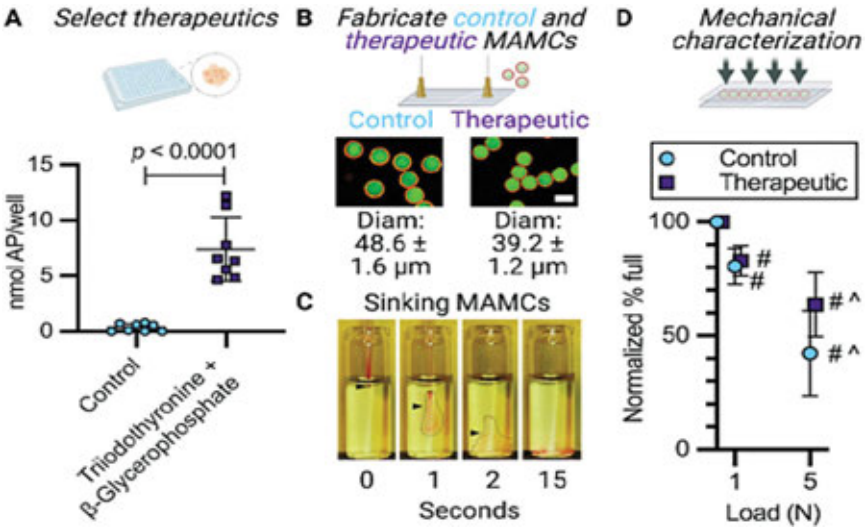

Figure 1. Development of mechanically activated microcapsules (MAMCs) containing osteogenic therapeutics—triiodothyronine and ß-glycerophosphate. **(A)** Alkaline phosphatase (AP) activity 2 weeks after a single dose of osteogenic agents to MSC pellets. **(B)** Fabricated MAMCs with and without osteogenic agents. Scale bar = 50 μm. **(C)** Sinking timeline in saline. **(D)** Mechanical characterization of MAMCs. #, ^ $p < 0.05$ compared to unloaded MAMCs, or MAMCs loaded to 1N, respectively (within the same condition).

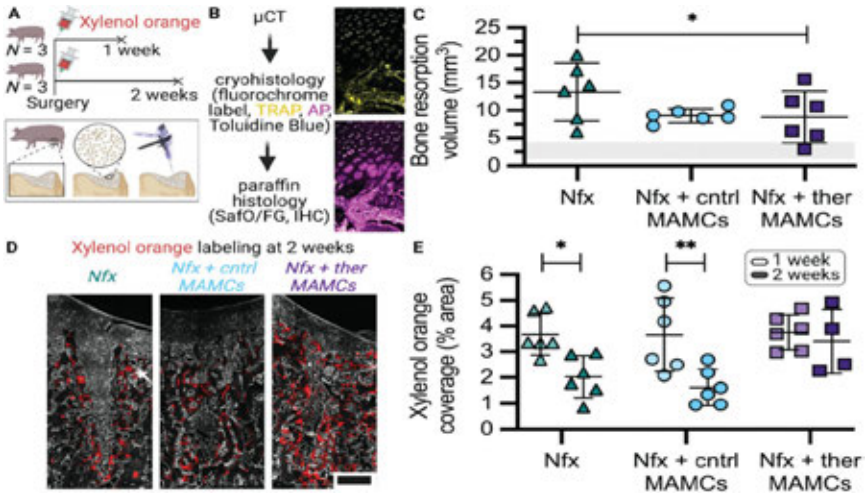

Figure 2. In vivo assessment of MAMCs containing osteogenic therapeutics to preserve bone structure after nanofracture. **(A)** Study and surgical outlines, respectively. **(B)** Outcome measures. TRAP: tartrate resistant acid phosphatase (yellow), AP: alkaline phosphatase (magenta). **(C)** Volumetric bone resorption after 2 weeks as assessed by μCT. Shaded region depicts range of values at 1 week. n = ± defects/condition. * $p < 0.05$. **(D)** Representative mineral labeling after 2 weeks. Scale bar = 1 mm. (E) Xylenol orange coverage near nanofracture hole at 1 week and 2 weeks post-labeling. n = 4-6 defects/condition per time. * $p < 0.05$, ** $p < 0.01$.

control groups, while label intensity was maintained with therapeutic MAMCs at this time (Figure 2E).

Discussion

Because mineral label incorporation is expected to occur over a 48 hr period post-injection, labeling coverage should be similar at later time points, unless label resorption is occurring. In our study, we observed a decrease in xylenol orange coverage in the Nfx alone, and NFx + control MAMCs group from the 1 to 2-week time point. However, the therapeutic MAMCs protected against this loss in label coverage. The intra-group variability observed for the therapeutic MAMC group may be attributed to the retention of the MAMCs within the defects. MAMCs were delivered within a saline solution and could have theoretically left the defect space after Nfx. We were unable to assess MAMC retention in this model, because of the overlying repair tissue. Future studies will ensure MAMC localization by incorporating these drug carriers within a scaffold or crosslinked hydrogel carrier material.

Significance

These data support the use of MAMCs for therapeutic delivery in load bearing environments, and the implementation of bone fluorochrome labeling to elucidate dynamic bony changes in large animals. This is the first assessment of therapeutic MAMCs in a large animal model.

Acknowledgements

This work was supported by the Department of Veterans' Affairs (I01 RX003375), the NSF (CMMI: 15-48571), and the NIH/NIAMS (R01 AR071340, T32 AR007132, P30 AR069619 F31 AR077395). The authors would also like to thank Marrow Access Technologies for donating the SmartShot® devices, and the ULAR staff for their assistance with animal care.

References

1. Zlotnick, HM, Locke, RC, Stoeckl, BD, *et al.* Marked differences in local bone remodeling in response to different marrow stimulation techniques in a large animal. *European Cells and Materials* 2021; 41, 546–557.

2. Mueller MB, Fischer M, Zellner J, *et al.* Hypertrophy in mesenchymal stem cell chondrogenesis: effect of TGF-beta isoforms and chondrogenic conditioning. *Cells Tissues Organs* 2010;192(3):158-66.

3. Peredo AP, Jo YK, Duan G, *et al.* Mechano-activated biomolecule release in regenerating load-bearing tissue microenvironments. *Biomaterials* 2021; 265:120255.

4. Dyment NA, Jiang X, Chen L, *et al.* High-Throughput, Multi-Image Cryohistology of Mineralized Tissues. J*ournal of Visualized Experiments* 2016;